Chemical Engineering Journal 160 (2010) 207–214

Contents lists available at ScienceDirect

Chemical Engineering Journal

journal homepage: www.elsevier.com/locate/cej

Propane/propylene separation with Li-exchanged zeolite 13X

Carlos A. Grande [a], Jorge Gascon [b], Freek Kapteijn [b], Alírio E. Rodrigues [a,*]

[a] Laboratory of Separation and Reaction Engineering (LSRE), Associate Laboratory LSRE/LCM, Department of Chemical Engineering, Faculty of Engineering, University of Porto, Rua Dr. Roberto Frias, s/n, 4200-465 Porto, Portugal
[b] Catalysis Engineering, Chemical Engineering Department, Delft University of Technology, Julianalaan 136, 2628 BL, Delft, The Netherlands

ARTICLE INFO

Article history:
Received 26 January 2010
Received in revised form 18 March 2010
Accepted 19 March 2010

Keywords:
Propane–propylene separation
Pressure swing adsorption
Zeolite
LiX

ABSTRACT

Selective adsorption of propylene from mixtures with propane over a lithium-exchanged zeolite 13X has been studied.

Adsorption equilibrium of pure gases has been evaluated at three different temperatures by volumetric and gravimetric methods. Propylene is adsorbed preferentially over propane, particularly at low pressures. Adsorption equilibrium can be well described with the multi-site Langmuir and the Virial models. At 1 bar and 323 K, the amount adsorbed of propylene is 2.5 mol/kg while the loading of propane is 2.0 mol/kg.

The dynamic behavior of the sample has also been evaluated on the bench scale in a fixed-bed for binary breakthrough performance. Macropore adsorption controls the diffusion process within the extrudates of the zeolite. The mathematical model could satisfactorily predict the behavior of the bed. The data obtained in this work allows to model any adsorption-based process for propane/propylene separation, like vacuum pressure swing adsorption and simulated moving bed.

1. Introduction

One of the most energy intensive separation processes in chemical industry is propane–propylene separation. These gases are separated in a distillation tower (C_3 splitter) running with extremely low relative volatilities. Furthermore, propylene purity higher than 99.5% is required to comply "polymer-grade" propylene specifications. To achieve such high purities, the distillation tower contains a large number of theoretical plates and is operated with large reflux/feed ratios [1]. It is suggested in many reports that more selective methods can be employed to reduce energetic intensity of this separation [2–5]. In this context, in addition to energy integration in the distillation process, adsorption has been widely studied as one of the possible techniques since high selectivity towards propylene may be achieved with the aid of porous solids. In particular, vacuum pressure swing adsorption (VPSA) has been suggested since it can be operated at relatively high productivities reducing separation volume [6–21]. However, this application of VPSA is not traditional: the most adsorbed gas should be purified to extremely high purities. For this reason, different VPSA operation has been suggested (using a rinse step with propylene and not using a purge step with propane). Furthermore, to comply with 99.5% purity, adsorbents with extremely high selectivity towards propylene are required to minimize recycling and thus power consumption.

Since many researchers have faced this topic, there is a large database for adsorption of propane and propylene over porous solids. Among commercial adsorbents, all kind of zeolites, silica gel, activated carbons, etc. can be mentioned [22–33]. Other inorganic silica-containing materials like DD3R, SBA-15 and MCM-41 have also been tested as well as metal–organic frameworks [16,34–38]. Finally, several materials modified with Ag^+ and Cu^+ to promote π-complexation with C_3H_6 were also reported [8,11,12,15,37,39,40].

In this work we report experimental data obtained with a Li-exchanged zeolite 13X as a more selective adsorbent that allows an improved design of a VPSA unit for propane/propene separation. It is initially expected that lithium cations interact strongly with propylene increasing the selectivity towards this gas. Furthermore, we have compared volumetric and gravimetric adsorption equilibrium data measured in two different laboratories. Bench scale fixed-bed breakthrough curves demonstrate the separation performance of binary streams of these gases.

2. Experimental

2.1. Adsorbent synthesis

All chemicals were obtained from Sigma–Aldrich and were used without further purification.

* Corresponding author. Tel.: +351 22 508 1618; fax: +351 22 508 1674.
E-mail address: arodrig@fe.up.pt (A.E. Rodrigues).

1385-8947/$ – see front matter © 2010 Elsevier B.V. All rights reserved.
doi:10.1016/j.cej.2010.03.044

Table 1
Physical properties of the Li-modified zeolite 13X and column characteristics employed in the multicomponent breakthrough curves.

Column length [m]	0.85	Solid heat capacity [J/kg K]	900
Column radius [m]	0.0105	Wall density [kg/m^3]	8238
Column porosity, ε_c[a]	0.349/0.394	Wall heat capacity [J/kg K]	500
Adsorbent density, ρ_p [kg/m^3]	1192	Heat transfer coefficient [W/m^2 K]	80
Extrudate diameter [mm][b]	1.18	Overall heat transfer coefficient [W/m^2 K]	23
Pellet void, ε_p	0.39	C_3H_6 preexponential crystal diffusivity [m^2/s][c]	5.8×10^{-8}
Macropore volume [cm^3/g]	0.39	C_3H_6 diffusivity activation energy [J/mol][c]	23.8
Mean macropore size [μm]	0.5	C_3H_8 preexponential crystal diffusivity [m^2/s][c]	1.4×10^{-8}
Mean zeolite crystallite diameter [μm]	2.0	C_3H_8 diffusivity activation energy [J/mol][c]	21.1

[a] The two values of porosity refer to the two different layers of the column.
[b] Extrudates larger than 1.18 mm were employed at $z < 0.65$ m while extrudates larger than 0.6 mm were employed from 0.65 m $< z <$ 0.85 m.
[c] Crystal diffusion parameters of zeolite 13X were employed in the simulations [27].

Scanning electron microscopy (SEM) was measured in a JEOL JSM 6500F setup. A micrograph of the exchanged zeolite is shown in Fig. 1. The crystalline structures were analyzed by X-ray diffraction (XRD) using a Bruker-AXS D5005 with CuKα radiation. The samples were digested in duplo in a mixture of 1% HF and 1.25% H_2SO_4 for elemental analysis that was carried out with a plasma optical emission spectroscopy (ICP-OES) Perkin Elmer Optima 3000dv.

Preparation of the Li-modified zeolite 13X: 100 g of commercial zeolite 13X 3.2 mm extrudates (Sigma–Aldrich, Product Number 334359) were ion exchanged three times for 24 h at 298 K with a fresh solution 1 M of LiCl (1 l of fresh solution each time). The analysis (ICP-OES) of the obtained sample after ion exchange revealed a percentage of ion exchange of an 80%.

2.2. Adsorption equilibrium

A Micromeritics ASAP 2010 gas adsorption analyser (stainless steel version) was used to measure the adsorption isotherms of propane, and propylene on Li-13X at 323, 353 and 383 K, in the pressure range from 0.002 to 120 kPa. The samples were maintained at these temperatures using either water (323 K) or oil baths (353 and 383 K) around the sample cell. The instrument is equipped with turbo-molecular vacuum pumps and three different pressure transducers (0.13, 1.33 and 133 kPa) to enhance the sensitivity in the different pressure ranges. The static–volumetric technique was used to determine the volume of the gas adsorbed at different partial pressures: upon adsorption a pressure decrease was observed in the gas phase, allowing direct calculation of the amount adsorbed.

Prior to the adsorption measurements the samples were slowly degassed in situ in vacuum for 16 h at 383 K followed by 6 h at 523 K. The evacuation at 383 K allowed the adsorbed hydrocarbons and water to escape from the sample cell at lower temperatures.

Gravimetric adsorption equilibrium experiments of pure propane and propylene were performed in a magnetic suspension microbalance (Rubotherm, Germany). Measurements were performed with a mass of adsorbent of approximately 5 g to minimize errors of the measurements, which are already very small (±0.00002 g). Pressure was monitored with a pressure transducer with a range from 0 to 700 kPa (±0.14 kPa). An initial degassing of the sample was carried out under vacuum at 593 K overnight. Regeneration for different experiments was only performed under vacuum (<10^{-7} bar) at the desired temperature. Propane and propylene isotherms were measured at 323, 353 and 383 K. Reversibility of the isotherms was checked by measuring some desorption points. Propylene N25 (purity higher than 99.5%) and propane N35 (purity higher than 99.95%) supplied by Air Liquide (France) were employed in the experiments.

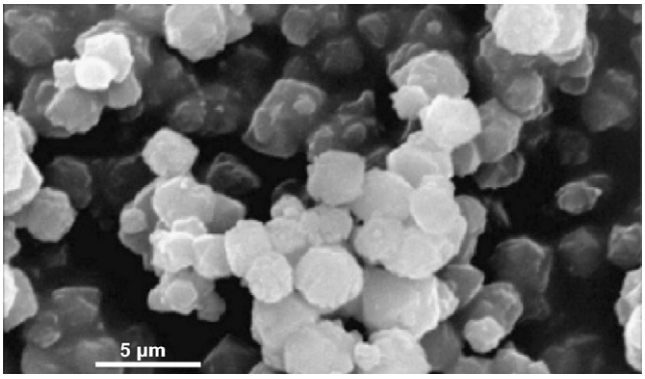

Fig. 1. SEM micrograph of the lithium-exchanged zeolite 13X.

2.3. Fixed-bed experiments

Binary breakthrough experiments were performed in a single-column VPSA unit [43]. Before packing the column, the adsorbent extrudates were ground. The particles with diameter larger than 1.18 mm were packed in the initial 0.65 m of the column while extrudates with diameters between 0.60 and 1.18 mm were packed in the last portion of the column: from 0.65 to 0.85 m. The properties of the column and adsorbent used are described in Table 1. The temperature in the centre of the column was measured with three different K-type thermocouples (Omega, UK) at three different bed heights (0.17, 0.42 and 0.67 m from feed inlet). Before the experiments, the sample was degassed overnight under helium flow at 593 K. The complete set of experimental conditions of the experiments is detailed in Table 2. The pressure in the column is controlled by a backpressure controller (Bronkhorst, Netherlands). Propane, propylene and helium are fed to the column through independent mass flow controllers (Hastings, USA). The gas exiting the column was mixed with a known amount of a tracer gas (ethane) to calculate individual gas flowrates. During each experiment, samples of the outlet stream were stored in the loops of a multi-port valve system and afterwards analyzed by a gas chromatograph (Chrompack CP9001, Netherlands) equipped with TCD and FID detectors (thermal conductivity detector and flame ionization detector).

Table 2
Experimental conditions employed in the breakthrough experiments with Li-modified zeolite 13X.

	Run			
	1	2	3	4
Temperature [K]	353	353	353	353
Pressure [bar]	2.5	2.5	2.5	2.5
Flowrate [dm^3(STP)/min]	1.40	2.11	1.18	1.14
C_3H_6 molar fraction	0.504	0.479	0.161	0.720
C_3H_8 molar fraction	0.000	0.521	0.839	0.280
He molar fraction	0.496	0.000	0.000	0.000

3. Theoretical

Adsorption equilibrium of pure components was fitted to the multi-site Langmuir model [41]. The multicomponent extension of this model is:

$$\frac{q_i}{q_{\max,i}} = K_i P \left(1 - \sum \frac{q_i}{q_{\max,i}}\right)^{a_i} \quad (1)$$

where $q_{\max,i}$ is the maximum amount adsorbed and a_i is the number of sites occupied per molecule. The adsorption constant (K_i) has an exponential temperature dependence described by:

$$K_i = K_i^0 \exp\left(\frac{-\Delta H_i}{RT_s}\right) \quad (2)$$

where K_i^0 is the adsorption constant at infinite temperature, R is the universal gas constant and $(-\Delta H_i)$ is the isosteric heat of adsorption, both for component i.

Pure gas isotherms were employed to determine these four constants ($q_{\max,i}$, a_i, K_i^0 and ΔH_i) for each gas and then employ them in the prediction of multicomponent adsorption equilibrium. The saturation capacity of each component was imposed by the thermodynamic constraint $a_i q_{\max,i}$ = constant.

Another flexible model employed to correlate the experimental data is the Virial equation [18,19]. This model is thermodynamically correct and has analytical expressions for prediction of multicomponent behavior. The model is represented by:

$$P = \frac{q}{H} \exp(Aq + Bq^2 + \cdots) \quad (3)$$

In this equation, A and B are Virial coefficients, and H is the Henry constant. The Henry constant is related to the solid temperature (T_s) through the Van't Hoff equation:

$$H = H_\infty \exp\left(\frac{-\Delta H}{RT_s}\right) \quad (4)$$

where H_∞ is the Henry constant at infinite temperature, $(-\Delta H)$ is the heat of adsorption at zero coverage. The temperature dependence of Virial coefficients is given by:

$$A = A_0 + \frac{A_1}{T}, \quad B = B_0 + \frac{B_1}{T} \quad (5)$$

Taqvi and LeVan [42] extended the Virial isotherm to multicomponent adsorption in a predictive mode as follows:

$$P_i = \frac{q_i}{H_i} \exp\left(\sum_{j=1}^{N} A_{ij} q_j + \sum_{j=1}^{N}\sum_{k=1}^{N} B_{ijk} q_j q_k\right) \quad (6)$$

with the mixing Virial coefficients (A_{ij} and B_{ijk}) calculated by [42]:

$$A_{ij} = \frac{A_i + A_j}{2} \quad (7)$$

$$B_{ijk} = \frac{B_i + B_j + B_k}{3} \quad (8)$$

The isotherm models employed in this work have a strong theoretical background [18,19,41] combined with a great flexibility for fitting experimental data. Virial model was already employed in the description of adsorption of gases on Li-modified adsorbents [52]. The Virial model has more parameters allowing a better description of experimental data. The fitting of both models to experimental data was performed using MATLAB (The MathWorks, Inc.). The minimization routine employed finds the minimum of the objective function using the Nelder–Mead Simplex Method of direct search.

The breakthrough curves were simulated using a mathematical model comprising material, momentum and energy balances. The following assumptions were made in order to derive the necessary conservation equations [43]:

1. Ideal gas behavior inside the column.
2. No mass, heat or velocity variations in the radial direction.
3. Axial dispersed plug flow.
4. External mass and heat transfer resistances expressed with the film model.
5. Bidisperse adsorbent particle: macropore and micropore mass transfer resistances expressed with the linear driving force (LDF) model.
6. No temperature gradients inside each particle.
7. The column is packed with two layers of adsorbent: larger cylinders with diameter larger than 1.18 mm (assumed as infinite cylinders) followed by smaller cylinders with diameters between 0.60 and 1.18 mm (considered as spheres). Inside each layer, porosity is considered constant.

The mass balance for each component in the gas phase is given by:

$$\varepsilon_c \frac{\partial C_i}{\partial t} = \varepsilon_c \frac{\partial}{\partial z}\left(D_{ax} C_T \frac{\partial y_i}{\partial t}\right) - \frac{\partial (u_0 C_i)}{\partial z} - (1-\varepsilon_c)\frac{a' k_{fi}}{Bi_i/5+1}(C_i - \overline{c_i}) \quad (9)$$

where C_i is the gas phase concentration, D_{ax} is the axial dispersion coefficient, u_0 is the superficial velocity, ε_c is the column porosity, y_i is the molar fraction, k_{fi} is the film mass transfer resistance, $Bi_i = R_p k_{fi}/(\varepsilon_p D_{p,i})$ is the Biot number and $\overline{c_i}$ is the averaged concentration in the macropores, all valid for component i, while C_T is the total gas concentration and a' is the pellet specific area.

We have assumed a LDF model for the mass transfer rate from the gas phase to the macropores. In this work, two different layers are placed in the column: an initial layer where extrudates can be considered as cylinders followed by a second layer where cylinders are shorter and can be approximated to spheres. The mass balances for these two layers are:

$$\varepsilon_p \frac{\partial \overline{c_i}}{\partial t} + \rho_p \frac{\partial \langle \overline{q_i} \rangle}{\partial t} = \varepsilon_p \frac{8 D_{p,i}}{R_p^2} \frac{1}{1 + 5/Bi_i}(C_i - \overline{c_i}) \quad \text{for } z < 0.65\ \text{m}$$

$$\varepsilon_p \frac{\partial \overline{c_i}}{\partial t} + \rho_p \frac{\partial \langle \overline{q_i} \rangle}{\partial t} = \varepsilon_p \frac{15 D_{p,i}}{R_p^2} \frac{1}{1 + 5/Bi_i}(C_i - \overline{c_i}) \quad \text{for } z \geq 0.65\ \text{m} \quad (10)$$

where $D_{p,i}$ is the pore diffusivity, R_p is the extrudate radius, ρ_p is the particle density, ε_p is the particle porosity and $\langle \overline{q_i} \rangle$ is the extrudate averaged adsorbed phase concentration.

The LDF equation for the crystals averaged over the entire extrudates is expressed by:

$$\frac{\partial \langle \overline{q_i} \rangle}{\partial t} = \frac{15 D_{c,i}}{r_c^2}\left(q_i - \langle \overline{q_i} \rangle\right) \quad (11)$$

where $D_{c,i}$ is the crystal diffusivity, r_c is the crystal radius and q_i is the adsorbed phase concentration in the equilibrium state.

In the momentum balance we have considered that the pressure drop and velocity change are related through the Ergun equation, defined by:

$$-\frac{\partial P}{\partial z} = \frac{150\mu(1-\varepsilon)^2}{\varepsilon_c^3 d_p^2} u_0 + \frac{1.75(1-\varepsilon)\rho_g}{\varepsilon_c^3 d_p} |u_0| u_0 \quad (12)$$

where P is the total gas pressure, μ is the gas viscosity, ρ_g is the gas density and d_p is the particle diameter.

The energy balance in the gas phase is:

$$\frac{\partial}{\partial z}\left(\lambda \frac{\partial T_g}{\partial z}\right) - u_0 C_{g,T} C_p \frac{\partial T_g}{\partial z} + \varepsilon_c R_g T_g \frac{\partial C_{g,T}}{\partial t} - (1-\varepsilon_c) a_p h_f (T_g - T_p) - \frac{4 h_w}{d_{wi}}(T_g - T_w) - \varepsilon_c C_{g,T} C_v \frac{\partial T_g}{\partial t} = 0 \quad (13)$$

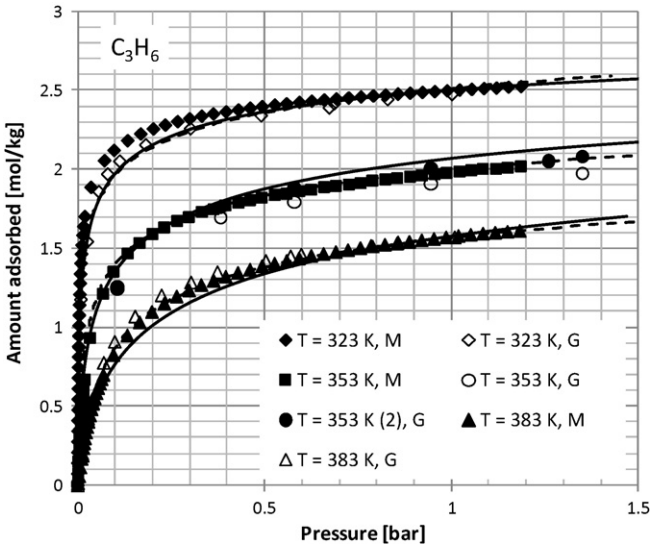

Fig. 2. Adsorption equilibrium of propylene in Li-modified zeolite 13X measured by volumetric and gravimetric techniques at 323 K (♦, ◊), 353 K (■, ●, ○) and 383 K (▲, △). Key: M represents volumetric while G means gravimetric. Solid lines correspond to the multi-site Langmuir model and dotted lines are the Virial model.

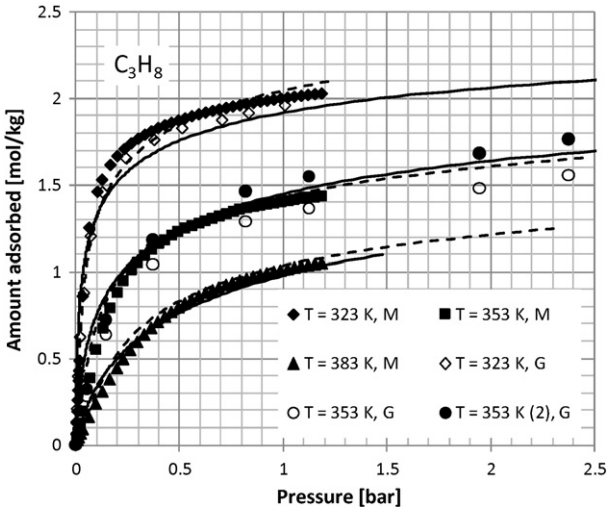

Fig. 3. Adsorption equilibrium of propane in Li-modified zeolite 13X measured by volumetric and gravimetric techniques at 323 K (♦, ◊), 353 K (■, ●, ○) and 383 K (▲). Key: M represents volumetric while G means gravimetric. Solid lines correspond to the multi-site Langmuir model and dotted lines are the Virial model.

with T_g, T_p and T_w respectively as the gas, particle and wall temperatures; C_v and C_p as the gas molar specific heat at constant volume and pressure respectively; R_g as the ideal gas constant; d_{wi} as the wall internal diameter, λ as the heat axial dispersion coefficient. The film heat transfer coefficient between the gas phase and the particle is represented by h_f, while the film heat transfer coefficient between the gas phase and the wall is represented by h_w.

As it is assumed that there are no temperature gradients inside a particle, the solid phase energy balance for the column is given by:

$$(1-\varepsilon_c)\left[\rho_p\sum_{i=1}^{n}\overline{q_i}C_{v,ads,i}+\rho_p C_{p,s}\right]\frac{\partial T_p}{\partial t}=(1-\varepsilon_c)\varepsilon_p R_g T_p\frac{\partial C_T}{\partial t}$$

$$+(1-\varepsilon_c)\rho_p\sum_{i=1}^{n}(-\Delta H)_i\frac{\partial\overline{q_i}}{\partial t}+(1-\varepsilon_c)a_p h_f(T_g-T_p) \quad (14)$$

where ρ_b is the bulk density of the bed, $C_{p,s}$ is the solid specific heat per unit sorbent mass and $(-\Delta H)_i$ is the isosteric heat of adsorption of component i.

Finally, for the energy balance of the column wall energy exchange with the gas phase inside the column and with the external environment is considered:

$$\rho_w C_{p,w}\frac{\partial T_w}{\partial t}=\alpha_w h_w(T_g-T_w)-\alpha_{w\ell}U(T_w-T_\infty) \quad (15)$$

where T_∞ is the external temperature, ρ_w is the wall density, $C_{p,w}$ is the wall specific heat per mass unit, U is the overall heat transfer coefficient and α_w and $\alpha_{w\ell}$ are defined by:

$$\alpha_w=\frac{d_{wi}}{e(d_{wi}+e)};\quad \alpha_{w\ell}=\frac{1}{(d_{wi}+e)\ln(d_{wi}+e/d_{wi})} \quad (16)$$

where e is the wall thickness.

Note that in Eqs. (9), (12)–(14) two different values of column porosity were employed to describe the different layers in the column. These values are listed in Table 1.

This mathematical model has already been used in the simulation of fixed-bed behavior and pressure swing adsorption (PSA) for propane–propylene separation showing very good agreement between predictions and experimental data [13,14,19]. All necessary correlations to calculate mass and heat transfer constants are given elsewhere [43]. The simulations were performed with *gPROMS* (PSE Enterprise, UK) using the orthogonal collocation on finite elements as the numerical method. The number of elements used was 70 with third order polynomials (two interior collocation points).

4. Results and discussion

4.1. Adsorption equilibrium

In this work, adsorption equilibrium isotherms of pure propane and propylene in the Li-exchanged zeolite 13X were determined using two different methods: volumetric and gravimetric. Adsorption isotherms of propane and propylene for 323, 353 and 383 K are reported in Figs. 2 and 3, respectively. Propylene is more selectively adsorbed than propane. This selectivity decreases with pressure; at low coverage, propylene is much more adsorbed than propane, demonstrating the high affinity of this adsorbent. At 1 bar and 323 K, the amount of propylene adsorbed was 2.5 mol/kg while the loading of propane was 2.0 mol/kg. Also, every isotherm has a considerable steepness that may result in important tempera-

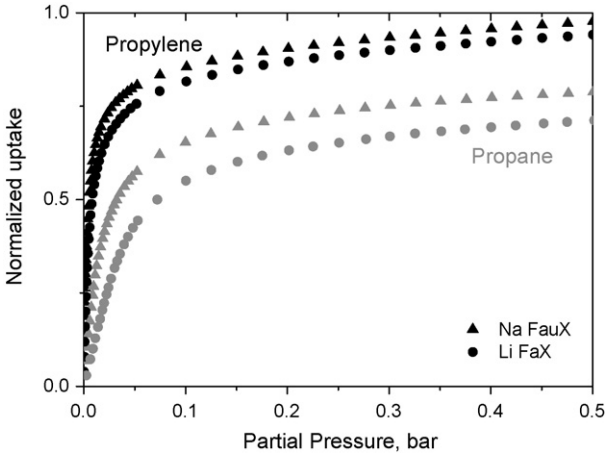

Fig. 4. Comparison between the adsorption isotherms of propane and propylene at 323 K for the same zeolite 13X (faujasite) extrudates before and after ion exchange with Li (Na and Li forms).

Table 3
Fitting parameters of multi-site Langmuir and Virial models for propane and propylene adsorption on Li-modified zeolite 13X at 323, 353 and 383 K.

Multi-site Langmuir	C_3H_6	C_3H_8
$q_{max,i}$ [mol/kg]	3.3179	3.0413
K_1^0 [mol/kg bar]	2.79×10^{-8}	2.00×10^{-8}
$-\Delta H$ [J/mol]	61454	58400
a_i	4.1249	4.500
Virial	C_3H_6	C_3H_8
K_∞ [mol/kg bar]	3.22×10^{-8}	1.15×10^{-5}
$-\Delta H$ [J/mol]	63761	39509
A_0 [kg/mol]	−3.1569	−1.3669
A_1 [kg K/mol]	1104.81	244.41
B_0 [kg/mol]^2	2.9628	5.4968
B_1 [kg K/mol]^2	−705.92	−1476.76

ture oscillations in VPSA operation; in the adsorption step, a large amount of heat is released reducing the bed capacity while in the blowdown/purge steps heat is consumed in propylene desorption lowering the temperature and increasing equilibrium and mass transfer difficulties. Fig. 4 compares the normalized isotherms of this sample with those for the Na-form of faujasite, zeolite 13X (extrudates before ion exchange) [27–33]. Propylene loading on Li-FAU at low pressure is quite similar to Na-FAU with a slightly smaller loading at higher pressures (4% at 0.5 bar). For propane, the loading on Li-FAU at low pressure is quite smaller than on Na-FAU (60% at 0.025 bar) with also a reduced loading at higher pressures (10% at 0.5 bar). With these loadings the propylene selectivity of Li-FAU is higher, especially at lower pressure.

An important result is that both methods, gravimetric and volumetric, tested in different laboratories yielded similar results. Additionally, with the gravimetric method, the adsorption equilibrium of two different portions of the same adsorbent was compared at 353 K. Deviations smaller than 10% occur with more important differences in the case of propane.

The solid lines in Figs. 2 and 3 correspond to the fitting using the multi-site Langmuir model, while the dotted lines correspond to the fitting of the Virial model. The estimated parameter values of both models are listed in Table 3. In both models, the heat of adsorption of propylene is quite similar and high. However, there are large differences in the value of the heat of adsorption of propane; much higher in the case of the multi-site Langmuir model than in the Virial equation. Since the isotherms are quite steep, and therefore the Henry zone pressure ranges of the isotherm are limited, it is very difficult to determine the behavior of the material at low pressures. For this reason, a closer analysis of the fitting at low pressures is necessary. This can be done in a Virial plot, as shown in Fig. 5. The multi-site Langmuir model cannot describe the low pressure data

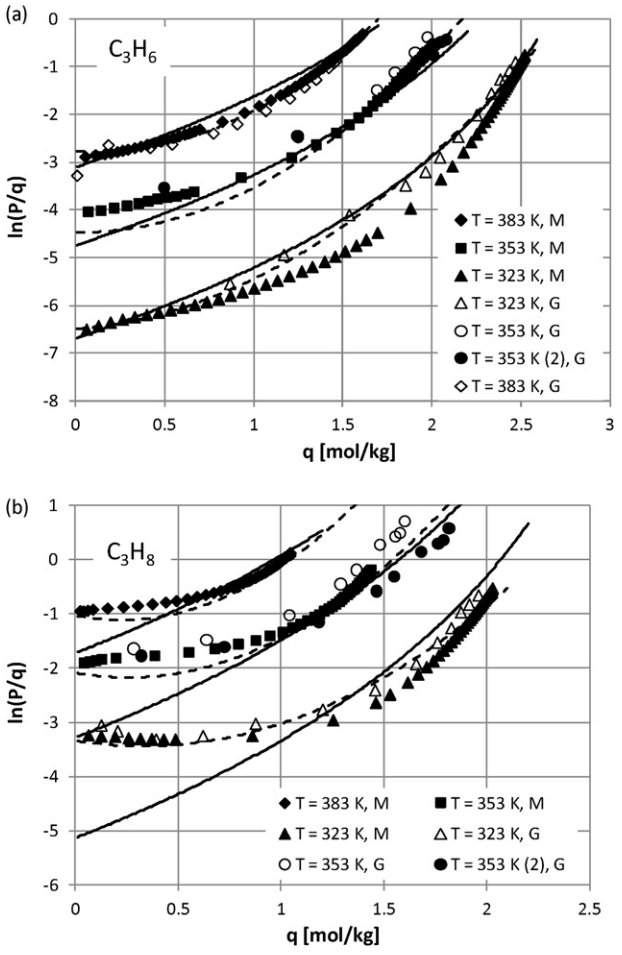

Fig. 5. Virial plots of propylene (a) and propane (b) for adsorption equilibrium on Li-modified zeolite 13X. Data was measured at 323 K (♦, ◊), 353 K (■, ●, ○) and 383 K (▲, △). Key: M represents volumetric while G means gravimetric. Solid lines correspond to the multi-site Langmuir model and dotted lines are the Virial model.

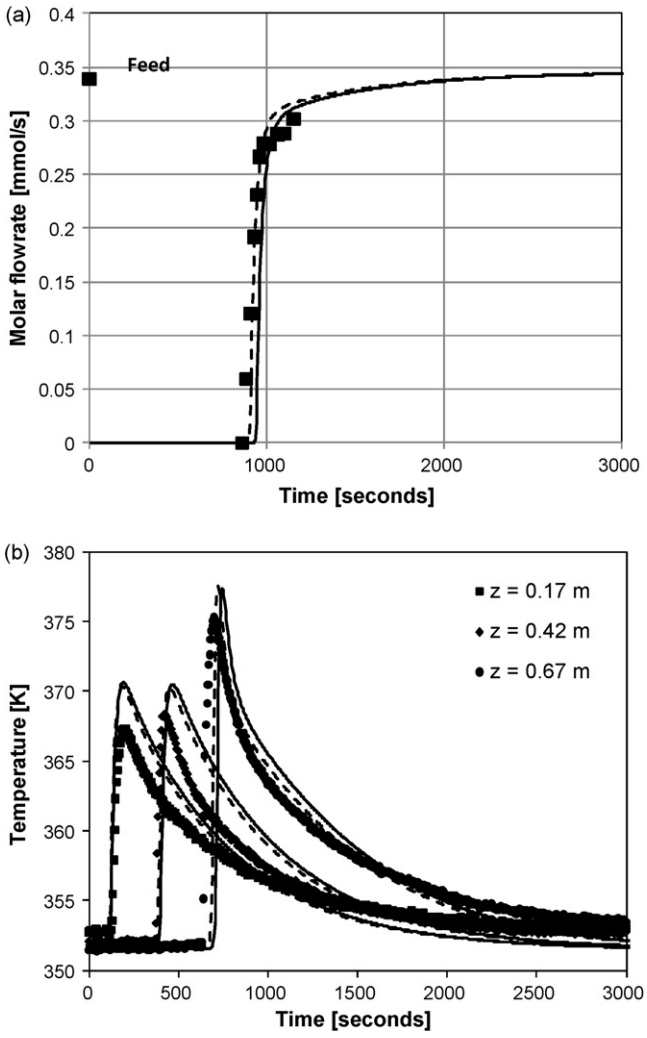

Fig. 6. Breakthrough curve of propylene in a mixture with helium in a fixed-bed filled with Li-modified zeolite 13X. Temperature: 353 K, pressure: 2.5 bar, C_3H_6 molar fraction: 0.50; feed flowrate: 1.01 SLPM (296 K, 1 bar). Solid lines correspond to the simulation using the adsorption equilibrium described by the multi-site Langmuir model while dotted lines represent the Virial model. (a) Exit molar flowrate and (b) temperature measured at three different positions along the column.

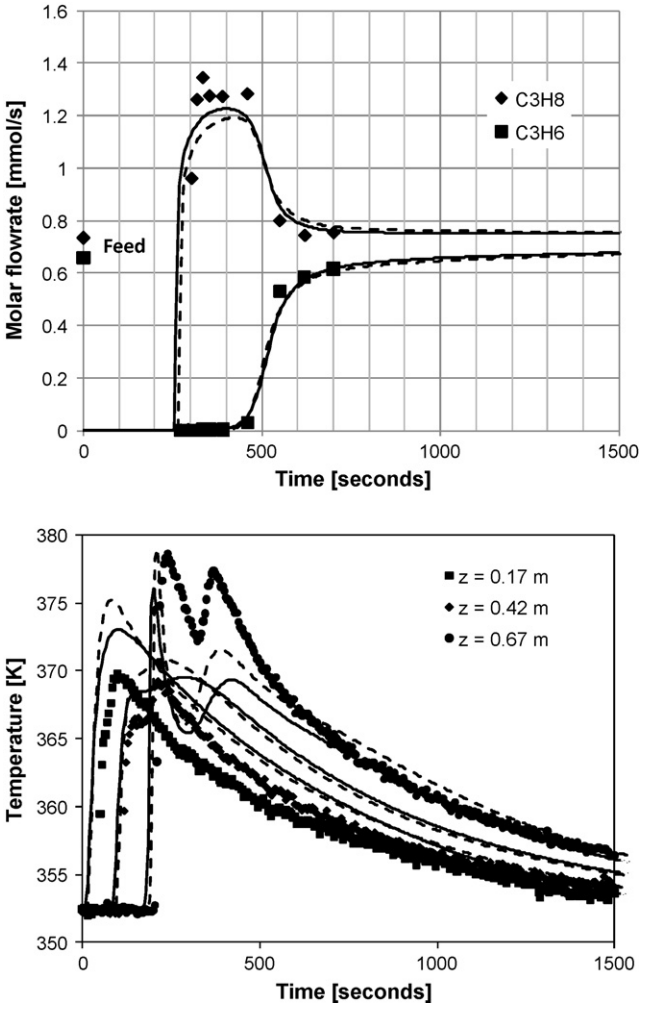

Fig. 7. Breakthrough curves of propylene/propane mixture in a fixed-bed filled with Li-modified zeolite 13X. Operating conditions of run 2 in Table 2. Solid lines correspond to the simulation using the adsorption equilibrium described by the multi-site Langmuir model while dotted lines represent the Virial model. (a) Exit molar flowrate and (b) temperature measured at three different positions along the column.

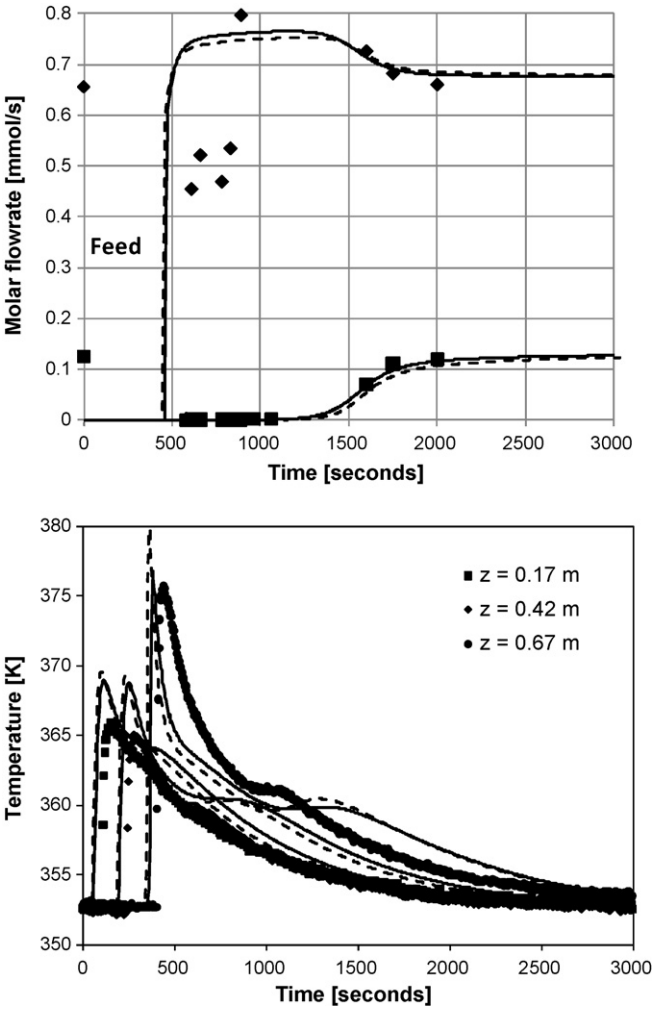

Fig. 8. Breakthrough curves of propylene/propane mixture in a fixed-bed filled with Li-modified zeolite 13X. Operating conditions of run 3 in Table 2. Solid lines correspond to the simulation using the adsorption equilibrium described by the multi-site Langmuir model while dotted lines represent the Virial model. (a) Exit molar flowrate and (b) temperature measured at three different positions along the column.

with enough accuracy. The fitting of the multi-site Langmuir model for propane isotherms is quite poor at low pressures: there are large deviations in all temperatures, reason why larger heats of adsorption are estimated. These large deviations may result in serious errors in the prediction of multicomponent adsorption equilibrium [44]. The errors of the prediction of adsorption equilibrium using the Virial model are significantly reduced at low pressures. However, it must be pointed out that this is in part due to the fact that more parameters are used to correlate the experimental data.

4.2. Breakthrough experiments

Adsorption processes are intrinsically transient. Selective adsorption of propylene takes place in the feed step, concentrating this gas in the column. To obtain high-purity propylene, this gas should be concentrated (normally by rinsing with pure propylene) and then recovered in regeneration steps (blowdown). At the same time, when the most adsorbed gas is removed, the column is partially regenerated to be prepared for the next cycle. To model and design an adsorption process, understanding how the mixture is separated in one column is essential. This is normally performed by analysis of breakthrough curves of the multicomponent mixture. Another important consideration is that in the VPSA cycles, the column contains very different concentrations of the gases. For this reason, it is important to perform several experiments to be sure that the mathematical model is able to predict the behavior of the mixture in a wide range of concentrations.

The first experiment performed was using a mixture of helium and propylene. Operating conditions of all experiments are detailed in Table 2. This first experiment contains only one adsorbate gas and helium that is considered as an inert and non-adsorbing gas. The main objective of this experiment is to confirm the capacity of the adsorbent that was determined by independent techniques (gravimetric and volumetric). Additionally, the coefficient of heat transfer from the extrudates to the wall (h_w) can be estimated. A unique value was obtained from this experiment and used in all other experiments. The results of this experiment are shown in Fig. 6 together with the temperature measured at the three different positions inside the column. The temperature peak in the last section of the column is the highest. This higher peak is caused by the smaller particles in the last section of the column (0.65–0.85 m) for which the internal diffusion process is much faster. Since more gas is adsorbed per unit of time, more heat is generated and the temperature of the column is increased. This is important evidence that the diffusion of both gases is controlled within the macropores of the adsorbent, since the crystallites of the zeolite are of the

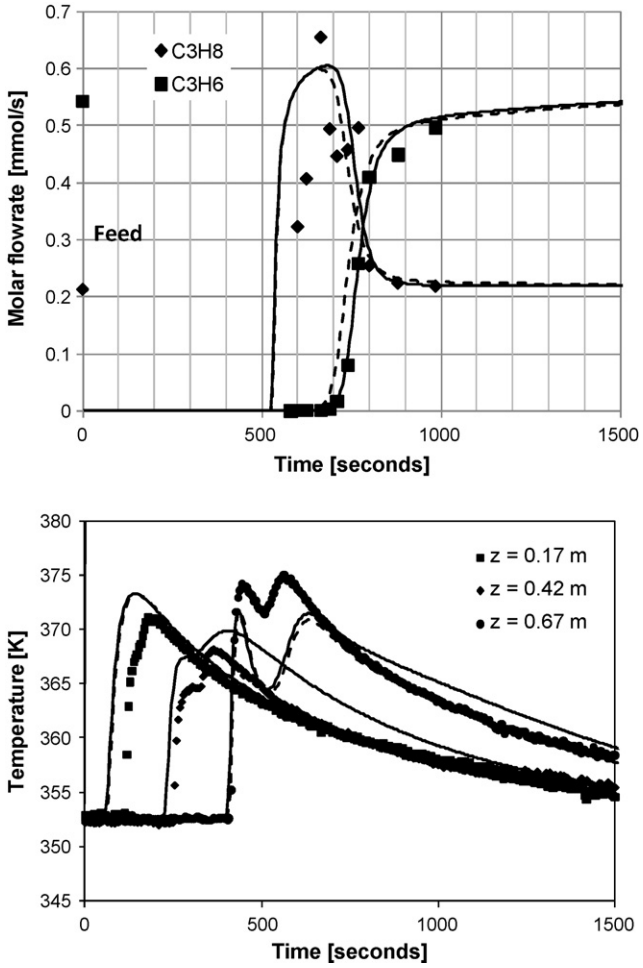

Fig. 9. Breakthrough curve of propylene + propane in a fixed-bed filled with Li-modified zeolite 13X. Operating conditions of run 4 in Table 2. Solid lines correspond to the simulation using the adsorption equilibrium described by the multi-site Langmuir model while dotted lines represent the Virial model. (a) Exit molar flowrate and (b) temperature measured at three different positions along the column.

same size in both cases. This result is in agreement with previous results obtained in zeolite 13X where macropore control was reported [27–33].

In Figs. 7–9 we report results obtained with three different mixtures of propane–propylene (experimental conditions are reported in Table 2). The solid lines correspond to the prediction of the mathematical model using the multi-site Langmuir isotherm while dotted lines correspond to the prediction based on the Virial isotherm. Despite the large deviations of the prediction of propane adsorption at low pressures, the multi-site Langmuir model can predict the behavior of the column with acceptable accuracy. The same accuracy is also found when the Virial model is employed. In all the experiments it was not possible to accurately describe the thermal behavior of the bed, particularly in the last portion of the column. However, the trends are well predicted by the model. In all breakthrough curves two consecutive temperature peaks are observed, corresponding to adsorption of propane followed by adsorption of propylene. These separate more from each other at low propylene concentrations.

The experimental data reported in this paper provide enough information to design and model adsorption processes such as vacuum pressure swing adsorption [45–48]. However, the steepness of the isotherms at partial pressures below 1 bar is quite high and may lead to a large power consumption of the process: blowdown should be carried out at very low pressures to remove sufficient amounts of propylene. Furthermore, the selectivity is not extremely high and thus an intense rinse with purified propylene should be carried out. The final conditions will result from a trade-off between required propylene purity and acceptable recovery. Nevertheless, a two-scheme VPSA processes in series can solve the problem [49]: the first VPSA process produce high-purity propylene and the second one enhances the overall recovery of the system.

An alternative adsorption-based process where this adsorbent can be employed is the simulated moving bed technology [50]. The gas phase separation of propane–propylene mixtures has already been simulated using zeolite 13X data [50] and similar results will be obtained with this adsorbent, since the equilibrium isotherms are quite similar and diffusion within porous structure is quite fast. The additional advantage of this adsorbent for SMB process is the higher ratio of Henry constants which will result in higher process productivity.

In terms of application, this adsorbent would be a very good candidate to remove either propane or/and propylene from air. Both propane and propylene are considered as volatile organic compounds (VOCs) and may be present in several locations reducing the air quality for humans [51]. This adsorbent presents several advantages over zeolite 13X: at lower temperatures it can remove more gas (either propane or propylene) and can be easily regenerated in a thermal swing adsorption (TSA) operation at lower temperatures. These two reasons would make the overall process more compact and more "environment friendly" because it consumes less energy.

5. Conclusions

Lithium modified zeolite 13X (Li-13X) sorbent was synthesized and characterized. Its adsorption properties for the separation of propane and propylene were evaluated in the temperature range from 323 to 383 K. Adsorption properties were determined by volumetric and gravimetric methods yielding similar results. Adsorption equilibrium isotherms indicate that propylene is preferentially adsorbed over propane, particularly at low coverages. At 1 bar and 323 K, the amount of propylene adsorbed is 2.5 mol/kg while the loading of propane was 2.0 mol/kg. The difference in loading between both gases is larger for Li-FAU than zeolite for 13X (Na-FAU). The isotherms of both gases are quite steep and heat of adsorption is higher than in commercial zeolite 13X. Binary breakthrough curves with different C_3 compositions were also evaluated. The separation zone increases when the molar fraction of propylene decreases. Due to the isotherm steepness and to the large heat of adsorption, this adsorbent will not be suitable for VPSA applications but might result attractive for TSA applications. In view of the fast adsorption kinetics of both gases and the acceptable capacity, this adsorbent might be also employed in Simulated Moving Bed (SMB) technology for C_3 separation. An alternative application would be the removal of traces propane or/and propylene from air; higher loading at low temperatures and faster regeneration make this adsorbent more suitable than commercial 13X zeolite.

Acknowledgment

JG acknowledges Senter Novem for financial support through the "EOS-LT Consortium Anorganische Membraan Technologie" (Lange termijn EOS-onderzoeksprogramma's), EOSLT-04008 managed by ECN.

References

[1] V. Gokhale, S. Hurowitz, J.B. Riggs, A comparison of advanced distillation control techniques for a propylene/propane splitter, Ind. Eng. Chem. Res. 34 (1995) 4413–4419.
[2] R.B. Eldridge, Olefin/paraffin separation technology: a review, Ind. Eng. Chem. Res. 32 (1993) 2208–2212.

[3] A. Mersmann, B. Fill, R. Hartmann, S. Maurer, The potential of energy saving by gas phase adsorption processes, Chem. Eng. Technol. 23 (2000) 937–944.
[4] R.B. Eldridge, F.A. Siebert, S. Robinson, Hybrid separations/distillation technology. Research opportunities for energy and emissions reduction. Available at: http://www1.eere.energy.gov/industry/chemicals (accessed 21.01.10).
[5] T. Ren, M. Patel, K. Blok, Energy efficiency and innovative emerging technologies for olefin production, in: Proceedings of the European Conference on Energy Efficiency in IPPC Installations, Vienna, Austria, 21–22 October, 2004.
[6] R. Ramachandran, L.H. Dao, B. Brooks, Method of producing unsaturated hydrocarbons and separating the same from saturated hydrocarbons, US Patent 5,365,011 (1994).
[7] H. Järvelin, J.R. Fair, Adsorptive separation of propane–propylene mixtures, Ind. Eng. Chem. Res. 32 (1993) 2201–2207.
[8] S.U. Rege, J. Padin, R.T. Yang, Olefin/paraffin separations by adsorption – Pi-complexation vs. kinetic separation, AIChE J. 44 (1998) 799–809.
[9] J. Padin, S.U. Rege, R.T. Yang, L.S. Cheng, Molecular-sieve sorbents for kinetic separation of propane/propylene, Chem. Eng. Sci. 55 (2000) 4525–4535.
[10] L.S Cheng, S.T. Wilson, Vacuum swing adsorption process for separating propylene from propane, US Patent 6,296,688 (2001).
[11] S.H. Cho, S.S. Han, J.N. Kim, N.V. Choudary, P. Kumar, S.G.T. Bhat, Adsorbents, method for the preparation and method for the separation of unsaturated hydrocarbons for gas mixtures, US Patent 6,315,816 (2001).
[12] N.V. Choudary, P. Kumar, V.R. Puranik, S.G.T. Bhat, Adsorbents, method for the manufacture thereof and process for the separation of unsaturated hydrocarbons from gas mixture, US Patent Application US2003/0097933A1 (2003).
[13] F.A. Da Silva, A.E. Rodrigues, Propylene/propane separation by VSA using commercial 13X zeolite pellets, AIChE J. 47 (2001) 341–357.
[14] F.A. Da Silva, A.E. Rodrigues, Vacuum swing adsorption for propylene/propane separation with 4A zeolite pellets, Ind. Eng. Chem. Res. 40 (2001) 5758–5774.
[15] R.T. Yang, J. Padin, S.U. Rege, Selective adsorption of alkenes using supported metal compounds, US Patent 6,423,881 (2001).
[16] D.H. Olson, Light hydrocarbon separation using 8-member ring zeolites, US Patent 6,488,741 (2002).
[17] S.M. Kuznicki, V.A. Bell, Olefin separation employing ETS molecular sieves, US Patent 6,517,611 (2003).
[18] S. Reyes, V.V. Krishnan, G.J. De Martin, J.H. Sinfelt, K.G. Strohmaier, J.G. Santiesteban, Separation of propylene from hydrocarbon mixtures, International Patent WO 03/080548 A1 (2003).
[19] C.A. Grande, A.E. Rodrigues, Propane–propylene separation by pressure swing adsorption using zeolite 4A, Ind. Eng. Chem. Res. 44 (2005) 8815–8829.
[20] C.A. Grande, N. Firpo, E.I. Basaldella, A.E. Rodrigues, Propane/propylene separation by SBA-15 and π-complexated Ag-SBA-15, Adsorption 11 (2005) 775–780.
[21] D.M. Ruthven, S.C. Reyes, Adsorptive separation of light olefins from paraffins, Micropor. Mesopor. Mater. 104 (2007) 59–66.
[22] W.K. Lewis, E. Gilliland, B. Chertow, W. Cadogan, Pure gas isotherms, Ind. Eng. Chem. 42 (1950) 1326–1332.
[23] G.R. Youngquist, J.L. Allen, J. Eisenberg, Adsorption of hydrocarbons by synthetic zeolites, Ind. Eng. Chem. Prod. Res. Develop. 10 (1971) 308–314.
[24] D.M. Ruthven, R.I. Derrah, Sorption in Davison 5A molecular sieves, Can. J. Chem. Eng. 50 (1972) 743–747.
[25] T.K. Ghosh, H. Lin, A.L. Hines, Hybrid adsorption–distillation process for separating propane and propylene, Ind. Eng. Chem. Res. 32 (1993) 2390–2399.
[26] S.N. Vyas, S.R. Patwardhan, S. Vijayalakshmi, K. Sri Ganesh, Adsorption of gases on carbon molecular sieves, J. Colloid Interf. Sci. 168 (1994) 275–280.
[27] F.A. Da Silva, A.E. Rodrigues, Adsorption equilibria and kinetics for propylene and propane over 13X and 4A zeolite pellets, Ind. Eng. Chem. Res. 38 (1999) 2434–2438.
[28] F. Rouquerol, J. Rouquerol, K. Song, Adsorption by Powders and Porous Solids, Academic Press, London, 1999.
[29] C.A. Grande, A.E. Rodrigues, Adsorption equilibria and kinetics of propane and propylene in silica gel, Ind. Eng. Chem. Res. 40 (2001) 1686–1693.
[30] C.A. Grande, C.E. Gigola, A.E. Rodrigues, Adsorption of propane and propylene in pellets and crystals of zeolite 5A, Ind. Eng. Chem. Res. 41 (2002) 85–92.
[31] C.A. Grande, V.M.T.M. Silva, C.E. Gigola, A.E. Rodrigues, Adsorption of propane and propylene onto carbon molecular sieve, Carbon 41 (2003) 2533–2545.
[32] R.T. Yang, Adsorbents. Fundamentals and Applications, J. Wiley, NJ, 2003.
[33] N. Lamia, L. Wolff, P. Leflaive, D. Leinekugel-le-Cocq, P.S. Gomes, C.A. Grande, A.E. Rodrigues, Equilibrium and fixed bed adsorption of 1-butene, propylene and propane over 13X zeolite pellets, Sep. Sci. Technol. 43 (2008) 1124–1156.
[34] W. Zhu, F. Kapteijn, J.A. Moulijn, M.C. den Exter, J.C. Jansen, Shape selectivity in adsorption of the all-silica DD3R, Langmuir 16 (2000) 3322–3329.
[35] J. Gascon, W. Blom, A. van Miltenburg, A.P.F. Ferreira, R.J. Berger, F. Kapteijn, Accelerated synthesis of all-silica DD3R and its performance in the separation of propylene/propane mixtures, Micropor. Mesopor. Mater. 115 (2008) 585–593.
[36] B.L. Newalkar, N.V. Choudary, P. Kumar, S. Komarneni, T.S.G. Bhat, Exploring the potential of mesoporous silica, SBA-15, as an adsorbent for light hydrocarbon separation, Chem. Mater. 14 (2002) 304–309.
[37] C.A. Grande, J.D.P. Araujo, S. Cavenati, N. Firpo, E.I. Basaldella, A.E. Rodrigues, New Pi-complexation adsorbents for propane/propylene separation, Langmuir 20 (2004) 5291–5297.
[38] N. Lamia, M. Jorge, M.A. Granato, F.A. Almeida Paz, H. Chevreau, A.E. Rodrigues, Adsorption of propane, propylene and isobutane on a metal–organic framework: molecular simulation and experiment, Chem. Eng. Sci. 64 (2009) 3246–3259.
[39] A. van Miltenburg, W. Zhu, F. Kapteijn, J.A. Moulijn, Adsorptive separation of light olefin/paraffin mixtures, Chem. Eng. Res. Des. 84 (2006) 350–354.
[40] A. van Miltenburg, J. Gascon, W. Zhu, F. Kapteijn, J.A. Moulijn, Propylene/propane mixture adsorption on faujasite sorbents, Adsorption 14 (2008) 309–321.
[41] T. Nitta, T. Shigetomi, M. Kuro-Oka, T. Katayama, An adsorption isotherm of multi-site occupancy model for homogeneous surface, J. Chem. Eng. Jpn. 17 (1984) 39–45.
[42] S.M. Taqvi, M.D. LeVan, Virial description of two-component adsorption on homogeneous and heterogeneous surfaces, Ind. Eng. Chem. Res. 36 (1997) 2197–2206.
[43] F.A. Da Silva, Cyclic adsorption processes: application to propane /propylene separation. Ph.D. Dissertation. University of Porto, Portugal, 1999.
[44] O. Talu, Needs, status, techniques and problems with binary gas adsorption experiments, Adv. Colloid Interf. Sci. 76–77 (1998) 227–269.
[45] D.M. Ruthven, S. Farooq, K.S. Knaebel, Pressure Swing Adsorption, VCH Publishers, New York, 1994.
[46] R.T. Yang, Gas Separation by Adsorption Processes, Butterworths, Boston, 1987.
[47] S. Sircar, Pressure swing adsorption, Ind. Eng. Chem. Res. 41 (2002) 1389–1392.
[48] R. Rota, P.C. Wankat, Intensification of pressure swing adsorption processes, AIChE J. 36 (1990) 1299–1312.
[49] A.E. Rodrigues, C.A. Grande, F. Poplow, Pressure swing adsorption. From fundamental data to plant design, in: Presentation in Fachausschuss Adsorption, Asselheim, Germany, 21–23 March, 2007.
[50] P. Sá Gomes, N. Lamia, A.E. Rodrigues, Design of a gas phase simulated moving bed for propane/propylene separation, Chem. Eng. Sci. 64 (2009) 1336–1357.
[51] G. Schürmann, K. Schäfer, C. Jahn, H. Hoffmann, M. Bauerfeind, E. Fleuti, B. Rappenglück, The impact of NO_x, CO and VOC emissions on the air quality of zurich airport, Atmos. Environ. 41 (2007) 103–118.
[52] F.N. Ridha, P.A. Webley, Anomalous Henry's Law behavior of nitrogen and carbon dioxide adsorption on alkali-exchanged chabazite zeolites, Sep. Purif. Technol. 64 (2009) 336–343.